

Tailoring of Deep-Red Luminescence in $\text{Ca}_2\text{SiO}_4\text{:Eu}^{2+**}$

Yasushi Sato,* Hideki Kato, Makoto Kobayashi, Takaki Masaki, Dae-Ho Yoon, and Masato Kakihana*

Abstract: We report a new dicalcium silicate phosphor, $\text{Ca}_{2-x}\text{Eu}_x\text{SiO}_4$, which emits red light in response to blue-light excitation. When excited at 450 nm, deep-red emission at 650 nm was clearly observed in $\text{Ca}_{1.2}\text{Eu}_{0.8}\text{SiO}_4$, the external and internal quantum efficiencies of which were 44 % and 50 %, respectively. The red emission from $\text{Ca}_{2-x}\text{Eu}_x\text{SiO}_4$ was strongly related to the peculiar coordination environments of Eu^{2+} in two types of Ca sites. The red-emitting $\text{Ca}_2\text{SiO}_4\text{:Eu}^{2+}$ phosphors are promising materials for next-generation, white-light-emitting diode applications.

The well-known crystal-site engineering has been often used to design inorganic functional materials.^[1,2] In the case of inorganic phosphors, from a crystallographic point of view, it is possible to customize the luminescence color of a given inorganic substance by employing the crystal-site engineering approach, as the luminescence wavelength changes according to the coordination environment at the site occupied by the luminescent center ion in the crystal. Of particular importance is that the luminescence wavelength of phosphors employing Eu^{2+} or Ce^{3+} as luminescent center ions changes greatly with the type of the crystal used as the parent.^[3,4] The controlled use of Eu^{2+} or Ce^{3+} ions in combination with a careful choice of the host crystal finds applications as solid-state lighting such as white light-emitting diodes (LEDs).^[5,6] For example, in the case of $\text{CaAlSiN}_3\text{:Eu}^{2+}$, which is used as a phosphor for solid-state lighting and for emitting a deep-red color owing to blue-light excitation, the luminescent center ion Eu^{2+} occupies a distinct calcium site and combines with five nitrogen atoms (thus, the coordination number is 5).^[7–9] The coordination environment of Eu^{2+} ions in $\text{CaAlSiN}_3\text{:Eu}^{2+}$ clearly indicates that the luminescence of $\text{CaAlSiN}_3\text{:Eu}^{2+}$ is

distinct and has a long wavelength (650 nm) in the deep-red domain.^[7–9] This is because the number of observed luminescence peaks is equivalent to the number of sites occupied by the luminescent center ions.

Unlike $\text{CaAlSiN}_3\text{:Eu}^{2+}$, in case where, a crystal involves two or more sites, at which luminescent center ions can occupy, it would be difficult, in general, for the required quantity of the luminescent center ions to occupy a desired site because of a possible size mismatch between the radius of the luminescent ion and that of the ion at the specific site. In other words, selective tuning of a desired emission color looks rather troublesome. However, if we take into consideration the fact that luminescent center ions will enter a less appropriate site by doping in a large concentration, we can expect observation of the selective emission from the luminescent center ions at the less appropriate site. This is because the emission from the great majority of the luminescent center ions occupying the normal sites would be largely depressed owing to the concentration quenching. Moreover, when focusing on Eu^{2+} ions, it should be noticed that Eu^{2+} plays a role not only as a luminescent center ion but also as one of the constituent ions building up a crystal structure. In view of these aspects, we chose $\text{Ca}_2\text{SiO}_4\text{:Eu}^{2+}$ as a model compound, where the host crystal of Ca_2SiO_4 involves several Ca sites with different coordination numbers,^[10–13] and Eu^{2+} ions can fully replace Ca^{2+} to form Eu_2SiO_4 .^[14] We demonstrate tailoring of the luminescence color in $\text{Ca}_2\text{SiO}_4\text{:Eu}^{2+}$ by imparting two roles to the luminescent center ion Eu^{2+} : forming a desired crystal structure and affording unreported deep-red luminescence to $\text{Ca}_2\text{SiO}_4\text{:Eu}^{2+}$ in a large concentration of Eu^{2+} .

According to our preliminary experiments, the phase transition β ($P2_1/n$ space group) \rightarrow α'_L ($Pna2_1$ space group) in the $\text{Ca}_{2-x}\text{Eu}_x\text{SiO}_4$ system occurred between $x=0.1$ and 0.2 (Supporting Information, Figure S1). This is similar to the phase transition $\beta \rightarrow \alpha'_L$ in the $\text{Ca}_{2-x}\text{Sr}_x\text{SiO}_4$ system.^[15] Figure 1 shows X-ray diffraction (XRD) patterns of $\text{Ca}_{2-x}\text{Eu}_x\text{SiO}_4$ with x values of 0.20, 0.40, 0.60, and 0.80. Furthermore, we also performed Rietveld refinements of the crystal structures of $\text{Ca}_{2-x}\text{Eu}_x\text{SiO}_4$ with x values of 0.2–0.8 (Supporting Information, Figure S2 a–d). In the refinements, the occupancy of Eu^{2+} at the Ca(1n) or Ca(2n) sites ($n=1–3$) was fixed, which means that the Eu^{2+} ions were assumed to be uniformly distributed among the Ca(1n) or Ca(2n) sites. All the samples exhibited orthorhombic unit cells with the space group $Pna2_1$, which is similar to the crystal structure of the $\text{Ca}_{2-x}\text{Sr}_x\text{SiO}_4$ system.^[12] The lattice constants (a , b , and c) systematically increased from $a=2.04031(31)$ nm, $b=0.93019(14)$ nm, and $c=0.55454(8)$ nm to $a=2.08002(36)$ nm, $b=0.94034(16)$ Å, and $c=0.55784(10)$ Å, with x increasing from 0.2 to 0.8, implying the incorporation of Eu^{2+} ions that were larger than

[*] Dr. Y. Sato,^[†] Prof. Dr. H. Kato, Dr. M. Kobayashi, Prof. Dr. M. Kakihana
Institute of Multidisciplinary Research for Advanced Materials
Tohoku University, Sendai 980-8577 (Japan)
E-mail: satoy@tagen.tohoku.ac.jp
kakihana@tagen.tohoku.ac.jp

Prof. Dr. T. Masaki, Prof. Dr. D. H. Yoon
School of Advanced Materials Science and Engineering
Sungkyunkwan University, Suwon 440-746 (Republic of Korea)

[†] Present address: Department of Chemistry, Faculty of Science
Okayama University of Science, Okayama 700-0005 (Japan)

[**] This work was partially supported by a Grant-in-Aid for Scientific Research on Innovative Areas of “Fusion Materials: Creative Development of Materials and Exploration of Their Function through Molecular Control” (No. 2206) from the Ministry of Education, Culture, Sports, Science and Technology (Japan) (MEXT).

Supporting information for this article is available on the WWW under <http://dx.doi.org/10.1002/anie.201402520>.

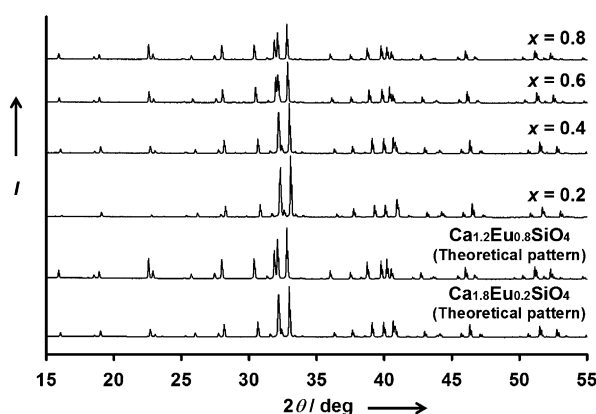


Figure 1. XRD patterns of $\text{Ca}_{2-x}\text{Eu}_x\text{SiO}_4$ with Eu^{2+} content (x) equal to 0.2, 0.4, 0.6, and 0.8. Theoretical XRD patterns of $\text{Ca}_{1.8}\text{Eu}_{0.2}\text{SiO}_4$ and $\text{Ca}_{1.2}\text{Eu}_{0.8}\text{SiO}_4$ obtained by Rietveld refinements (Supporting Information, Figure S2 a, d) are also shown as references.

Ca^{2+} into the α'_L - Ca_2SiO_4 lattice. Furthermore, the Rietveld refinements revealed that the estimated Eu^{2+} concentrations gradually increased not only from 9.63 to 36.45 mol % at the $\text{Ca}(1n)$ sites, but also from 0.37 to 3.55 mol % at the $\text{Ca}(2n)$ sites as x increased from 0.2 to 0.8. Thus, in the α'_L - $\text{Ca}_2\text{SiO}_4:\text{Eu}^{2+}$ structure, Eu^{2+} ions occupied both types of Ca sites as more Eu^{2+} was added.

Photoluminescence (PL) spectra of $\text{Ca}_2\text{SiO}_4:\text{Eu}^{2+}$ ($x = 0.1$ and 0.2) phosphors excited at 365 nm are shown in the Supporting Information, Figure S3. The sample with $x = 0.1$ exhibited a strong green emission with maximum intensity at approximately 510 nm, which was similar to those in previous studies.^[16,17] The transformation from the β to the α'_L phase was accompanied by a significant shift in the maximum emission wavelength from 510 to 550 nm. This change in the emission color can be directly related to the different coordination environments of the Eu^{2+} ions between the β - and α'_L - Ca_2SiO_4 phases.

Furthermore, it is worth noting that the emission colors were apparently shifted from green-yellow to deep-red with increasing Eu^{2+} content as x was varied from 0.2 to 0.6 or 0.8, even though all the host compounds remained in the α'_L - Ca_2SiO_4 phase. Figure 2 shows the emission spectra of

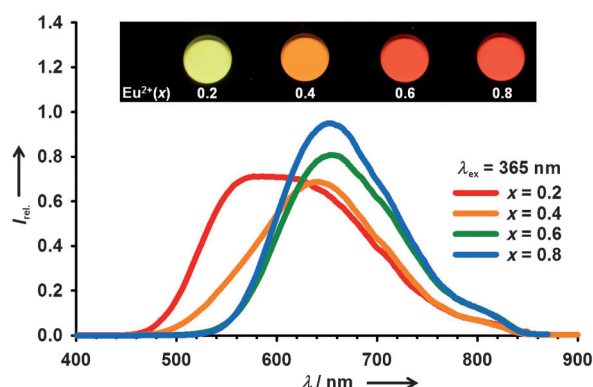


Figure 2. Emission spectra ($\lambda_{\text{ex}} = 365$ nm) of $\text{Ca}_{2-x}\text{Eu}_x\text{SiO}_4$ with Eu^{2+} content (x) equal to 0.2, 0.4, 0.6, and 0.8. Inset: photographs of these samples upon photo-excitation at 365 nm.

$\text{Ca}_2\text{SiO}_4:\text{Eu}^{2+}$ ($x = 0.2, 0.4, 0.6$, and 0.8) phosphors excited at 365 nm, along with inset photographs of the samples. For the sample with $x = 0.2$, the emission band became broader in the range from 460 to 840 nm, indicating that the emission band was mainly composed of two bands, that is, one band at a wavelength below 600 nm and another band at a wavelength above 600 nm. With further increases in the Eu^{2+} content, the shape of emission band was apparently changed. In particular, the samples with $x = 0.6$ and 0.8 exhibited broad emission bands peaking at around 650 nm.^[18] These changes imply that there were mainly two different emission centers in the α'_L - Ca_2SiO_4 lattice, as was the case with α' - $\text{Sr}_2\text{SiO}_4:\text{Eu}^{2+}$.^[19,20] The significant shifts from green-yellow to deep-red emission could therefore be related to a change in the emission center between the $\text{Ca}(1n)$ and $\text{Ca}(2n)$ sites. We had expected to assign the green-yellow emission to the $4f^7 \rightarrow 4f^65d^1$ transition of Eu^{2+} in the $\text{Ca}(1n)$ sites because of the preferential replacement with Eu^{2+} activators at the $\text{Ca}(1n)$ sites.^[17] However, with increasing Eu^{2+} content in the host compound, the green-yellow emission should disappear as a result of concentration quenching of Eu^{2+} emission from the $\text{Ca}(1n)$ sites. On the other hand, the Eu^{2+} concentration in the $\text{Ca}(2n)$ sites was approximately 3.55 mol % for the $x = 0.8$ sample, implying that this Eu^{2+} concentration was valid for the emission from Eu^{2+} in these sites. Therefore, the red emission could also be assigned to the $4f^7 \rightarrow 4f^65d^1$ transition of Eu^{2+} in the $\text{Ca}(2n)$ sites.

Figure 3 shows the emission spectrum of the $\text{Ca}_{1.2}\text{Eu}_{0.8}\text{SiO}_4$ phosphor that was excited at 450 nm, as well as the corresponding excitation spectrum that was monitored

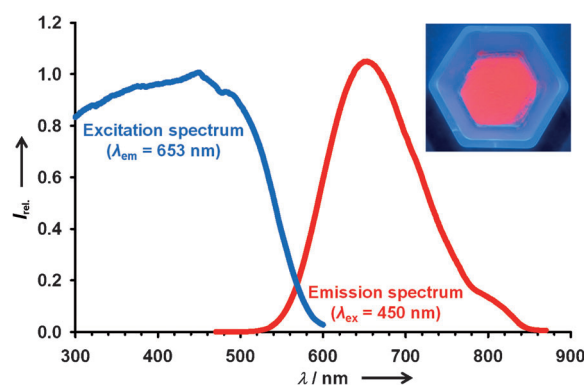


Figure 3. Emission ($\lambda_{\text{ex}} = 450$ nm) and excitation spectra of $\text{Ca}_{1.2}\text{Eu}_{0.8}\text{SiO}_4$ phosphor. The excitation spectrum was acquired by monitoring at the maximum emission wavelength ($\lambda_{\text{em}} = 650$ nm). Inset: the corresponding $\text{Ca}_{1.20}\text{Eu}_{0.80}\text{SiO}_4$ phosphor upon blue-light excitation with blue LEDs.

at 650 nm. The emission band of the sample was clearly visible at around 650 nm when the sample was excited at 450 nm. The external and internal quantum efficiencies (QEs) of $\text{Ca}_{1.2}\text{Eu}_{0.8}\text{SiO}_4$ were determined at 450 nm. The external QE was 44 % while the internal QE was 50 %. The characteristic of this red light emission was quite similar to those previously reported for $\text{CaAlSiN}_3:\text{Eu}^{2+}$ and $\text{Sr}_2\text{Si}_5\text{N}_8:\text{Eu}^{2+}$.^[7-9,21-23] The similarities among them were also confirmed by the compar-

ison with the chromaticity coordinate values of the International Commission on Illumination (CIE); the x and y values of $\text{Ca}_2\text{SiO}_4:\text{Eu}^{2+}$ with $x = 0.8$ were 0.64 and 0.35 under 450 nm light irradiation, which were comparable to those of $\text{CaAlSi}_3\text{N}_8:\text{Eu}^{2+}$ and $\text{Sr}_2\text{Si}_3\text{N}_8:\text{Eu}^{2+}$.^[8,22] The maximum excitation wavelength of the $\text{Ca}_{1.2}\text{Eu}_{0.8}\text{SiO}_4$ sample was observed to be around 450 nm, which is consistent with the emission wavelengths of commercial blue LEDs.

Along with the above measurements, we also observed the thermal quenching properties of $\text{Ca}_{1.2}\text{Eu}_{0.8}\text{SiO}_4$ in the excitation at 450 nm. Figure 4 shows a variation in emission intensity of $\text{Ca}_{1.2}\text{Eu}_{0.8}\text{SiO}_4$ at 650 nm as a function of heating temper-

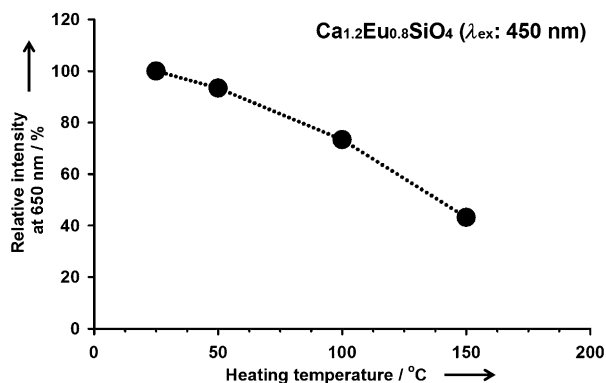


Figure 4. Variation in emission intensity (λ_{ex} : 450 nm) of $\text{Ca}_{1.2}\text{Eu}_{0.8}\text{SiO}_4$ at 650 nm, as a function of heating temperature. Emission intensity at each heating temperature was normalized by the initial intensity at room temperature.

ature. The emission intensity of $\text{Ca}_{1.2}\text{Eu}_{0.8}\text{SiO}_4$ at 650 nm gradually decreased with increasing heating temperature. The relative intensities at 100 and 150 °C (to the initial intensity at room temperature) were 73 % and 43 %, respectively. On the other hand, the maximum emission wavelength was shifted to lower wavelength with increasing heating temperature.

It can be seen that the $\text{Ca}_{1.2}\text{Eu}_{0.8}\text{SiO}_4$ phosphors possess 1) the broad emission band in the range from 520 to 840 nm and 2) the remarkable bump approximately at 800 nm, which leads to the lowering of the color quality and energy losses in the illumination application. Certainly, these features of the phosphors can be disadvantageous to the use of WLED applications. However, there have been a few reports of red-emitting oxide phosphors excited by blue light in previous studies.^[24,25] Therefore, we consider that the $\text{Ca}_2\text{SiO}_4:\text{Eu}^{2+}$ phosphors are interesting candidates as red-emitting oxide phosphors in white LEDs if its PL efficiency is further improved by the optimization of the preparation conditions such as use of flux reagent and heat-treatment.

As mentioned above, the deep-red emission observed in $\text{Ca}_2\text{SiO}_4:\text{Eu}^{2+}$ in the present work should be associated with the occupancies of Eu^{2+} ions in the $\text{Ca}(2n)$ sites. Based on the structural refinements we carried out for the α'_L - $\text{Ca}_2\text{SiO}_4:\text{Eu}^{2+}$ polycrystalline powders and those reported for α'_L - $\text{Ca}_2\text{SiO}_4:\text{Sr}^{2+}$ single crystals in previous publications,^[11,12] the average $\text{Ca}(\text{Eu}$ or $\text{Sr})\text{--O}$ bond length in the $\text{Ca}(2n)$ sites was much shorter than those in the $\text{Ca}(1n)$ sites.

Furthermore, the $\text{Ca}(2n)$ sites were relatively distorted because the bond lengths in these sites varied widely from the average bond length. Thus, it should be expected that the interactions between Eu^{2+} and O^{2-} (that is, nephelauxetic and crystal field effects for the 5d orbital of Eu^{2+}) at the $\text{Ca}(2n)$ sites were much stronger than those at the $\text{Ca}(1n)$ sites. Furthermore, the average $\text{Ca}(\text{Eu})\text{--O}$ bond lengths of $\text{Ca}(21)\text{--}\text{Ca}(23)$ sites were estimated to be 2.49–2.57 Å, which were almost similar to the average $\text{Ca}(\text{Eu})\text{--N}$ bond lengths (2.49 Å) of Ca sites in $\text{CaAlSi}_3\text{N}_8:\text{Eu}^{2+}$.^[8] This also indicates that deep-red emission from α'_L - $\text{Ca}_2\text{SiO}_4:\text{Eu}^{2+}$ originates from strong interactions between Eu^{2+} and O^{2-} owing to crystal field effects. Furthermore, the large amount of Eu^{2+} added to the initial composition of the $\text{Ca}_{2-x}\text{Eu}_x\text{SiO}_4$ system was sufficiently effective in promoting Eu^{2+} substitution in the $\text{Ca}(2n)$ sites because the Eu^{2+} ions preferentially occupied the large $\text{Ca}(1n)$ sites rather than the small $\text{Ca}(2n)$ sites in α'_L - Ca_2SiO_4 . More specifically, in the $\text{Ca}_{1.2}\text{Eu}_{0.8}\text{SiO}_4$ sample, the $\text{Ca}(1n)$ and $\text{Ca}(2n)$ site occupancies of Eu^{2+} ions were 91 and 9 %, respectively. Therefore, Eu^{2+} substitution in the $\text{Ca}(2n)$ sites by crystal-site engineering led to the deep-red emission at about 650 nm from α'_L - $\text{Ca}_2\text{SiO}_4:\text{Eu}^{2+}$.

In summary, we successfully prepared a series of $\text{Ca}_{2-x}\text{Eu}_x\text{SiO}_4$ ($\text{Ca}_2\text{SiO}_4:\text{Eu}^{2+}$) phosphors with Eu^{2+} content (x) ranging from 0.2 to 0.8 using crystal-site engineering approach. Based on the Rietveld refinement using X-ray diffraction data, the $\text{Ca}_2\text{SiO}_4:\text{Eu}^{2+}$ crystal structure was determined to be the orthorhombic α'_L phase ($Pna2_1$ space group) as x was increased from 0.2 to 0.8 and when Eu^{2+} ions were used as substitutes in both large $\text{Ca}(1n)$ sites and small $\text{Ca}(2n)$ sites. PL measurements revealed that the replacement with a large amount of Eu^{2+} ions was accompanied by a significant red-shift of the emission peak and deep-red light emission, peaking at 630–650 nm, in response to excitation at 450 nm. The external and internal QEs of $\text{Ca}_{1.2}\text{Eu}_{0.8}\text{SiO}_4$ were 44 % and 50 %. The red emission of the Eu^{2+} activators in $\text{Ca}_2\text{SiO}_4:\text{Eu}^{2+}$ was strongly related to the substituting Eu^{2+} ions in the small $\text{Ca}(2n)$ sites that possessed strong interactions between Eu^{2+} and O^{2-} . The red-emitting $\text{Ca}_2\text{SiO}_4:\text{Eu}^{2+}$ phosphors are thus promising materials for next-generation white LED applications.

Experimental Section

Polycrystalline $\text{Ca}_2\text{SiO}_4:\text{Eu}^{2+}$ powder was synthesized by a conventional solid-state reaction, using CaCO_3 , Eu_2O_3 , and SiO_2 powders as starting materials. These compounds were mixed in various ratios in ethanol using an agate mortar. The Eu^{2+} concentration (x) was varied from 0.2 to 0.4, 0.6, and 0.8 to produce a range of $\text{Ca}_{2-x}\text{Eu}_x\text{SiO}_4$ stoichiometries, and the resulting mixtures were calcined at 800–1100 °C in air for 6–12 h. Subsequently, the calcined powders were reground and mixed with small amounts of various chloride salts (which served as flux reagents),^[26] following which the powders were heat-treated in a tube furnace at 1000–1400 °C for 1–5 h under a flow of an Ar-H_2 ($\text{Ar}/\text{H}_2 = 96/4$) gas mixture.

The resulting $\text{Ca}_2\text{SiO}_4:\text{Eu}^{2+}$ powders were characterized by XRD (D2 PHASER, BrukerAXS) using $\text{Cu K}\alpha$ radiation. XRD patterns were collected using the continuous scan mode with a step interval of 0.02°. In the XRD measurements of samples containing higher concentrations of Eu, a significant increase in background signal was observed owing to sample fluorescence, and the XRD patterns in

these instances were therefore collected with optimized discriminator settings to suppress the fluorescence effect. We performed Rietveld analyses of the XRD patterns using the RIETAN-FP program to refine the structural parameters of all the samples.^[27] Additionally, the PL spectra of the $\text{Ca}_2\text{SiO}_4\text{:Eu}^{2+}$ powders were analyzed using a fluorescence spectrometer (F-4500, Hitachi). QE measurements and thermal quenching properties were performed using a fluorescence spectrometer (F-6500, JASCO) equipped with an integrating sphere (ISF-513).

Received: February 18, 2014

Revised: April 14, 2014

Published online: June 10, 2014

Keywords: crystal-site engineering · lanthanides · luminescence · phosphors · silicates

- [1] T. Watanabe, T. Kojima, T. Sakai, H. Funakubo, M. Osada, Y. Noguchi, M. Miyayama, *J. Appl. Phys.* **2002**, 92, 1518.
- [2] S.-T. Zhang, W.-J. Ji, L. Wang, L.-Y. Ding, Y.-F. Chen, Z.-G. Liu, *Solid State Commun.* **2009**, 149, 434–437.
- [3] P. Dorenbos, *J. Lumin.* **2000**, 91, 155–176.
- [4] P. Dorenbos, *J. Lumin.* **2003**, 104, 239–260.
- [5] E. F. Schubert, J. K. Kim, *Science* **2005**, 308, 1274–1278.
- [6] P. F. Smet, A. B. Parmentier, D. Poelman, *J. Electrochem. Soc.* **2011**, 158, R37.
- [7] K. Uheda, N. Hirotsaki, Y. Yamamoto, A. Naito, T. Nakajima, H. Yamamoto, *Electrochem. Solid-State Lett.* **2006**, 9, H22–H25.
- [8] X. Piao, K. Machida, T. Horikawa, H. Hanzawa, Y. Shimomura, N. Kijima, *Chem. Mater.* **2007**, 19, 4592–4599.
- [9] J. Li, T. Watanabe, H. Wada, T. Setoyama, M. Yoshimura, *Chem. Mater.* **2007**, 19, 3592–3594.
- [10] H. Saalfeld, *Am. Mineral.* **1975**, 60, 824–827.
- [11] M. Catti, G. Gazzoni, G. Ivaldi, *Acta Crystallogr. Sect. B* **1984**, 40, 537–544.
- [12] H. Itoh, F. Nishi, T. Kuribayashi, Y. Kudoh, *J. Mineral. Petrol. Sci.* **2009**, 104, 234–240.
- [13] J. Barbier, B. G. Hyde, *Acta Crystallogr. Sect. B* **1985**, 41, 383–390.
- [14] R. Verreault, *Phys. Kondens. Mater.* **1971**, 14, 37–54.
- [15] K. Fukuda, I. Maki, S. Ito, S. Ikeda, *J. Am. Ceram. Soc.* **1996**, 79, 2577–2581.
- [16] S.-W. Choi, S.-H. Hong, Y. J. Kim, *J. Am. Ceram. Soc.* **2009**, 92, 2025–2028.
- [17] Y. Y. Luo, D. S. Jo, K. Senthil, S. Tezuka, M. Kakihana, K. Toda, T. Masaki, D. H. Yoon, *J. Solid State Chem.* **2012**, 189, 68–74.
- [18] Each emission band comprised of three emission peaks at least in principle. This could be attributed to that the three different Ca(1n) or Ca(2n) sites (that is, each of the three emission centers) exist in the host lattice.
- [19] B. Lei, K. Machida, T. Horikawa, H. Hanzawa, *Jpn. J. Appl. Phys.* **2010**, 49, 095001.
- [20] Y. S. Won, S. S. Park, *J. Phys. Chem. Solids* **2010**, 71, 1742–1745.
- [21] R. Xie, N. Hirotsaki, T. Suehiro, F. Xu, M. Mitomo, *Chem. Mater.* **2006**, 18, 5578–5583.
- [22] X. Piao, T. Horikawa, H. Hanzawa, K. Machida, *Appl. Phys. Lett.* **2006**, 88, 161908.
- [23] T. Horikawa, X. Q. Piao, M. Fujitani, H. Hanzawa, K. Machida, *IOP Conf. Ser. Mater. Sci. Eng.* **2009**, 1, 012024.
- [24] N. Yamashita, *J. Electrochem. Soc.* **1993**, 140, 840.
- [25] N. Yamashita, *J. Lumin.* **1994**, 59, 195–199.
- [26] S. Tezuka, Y. Sato, T. Komukai, Y. Takatsuka, H. Kato, M. Kakihana, *Appl. Phys. Express* **2013**, 6, 072101.
- [27] F. Izumi, K. Momma, *Solid State Phenom.* **2007**, 130, 15–20.